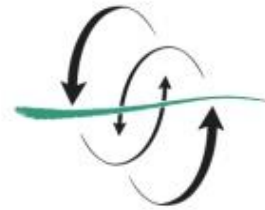


FACULTAD
DE CIENCIAS
DEL MAR



UNIVERSIDAD DE LAS PALMAS
DE GRAN CANARIA

**STUDY OF
ENVIRONMENTAL
RADIOACTIVITY IN LAS
CANTERAS BEACH**

**Ana del Carmen Arriola
Velásquez**

Curso 2015/2016

Dra. Alicia M. Tejera Cruz

Dr. Pablo Martel Escobar

Trabajo Fin de Título para la obtención
del título: Grado en Ciencias el Mar



STUDY OF ENVIRONMENTAL RADIOACTIVITY IN LAS CANTERAS BEACH

Datos personales del estudiante:

Ana del Carmen Arriola Velásquez

Grado en Ciencias del Mar

Curso 2015/2016

Universidad de Las Palmas de Gran Canaria

Facultad de Ciencias del Mar

e-mail: ana.arriola101@alu.ulpgc.es

Datos de los tutores:

Dra. Alicia M. Tejera Cruz

Universidad de Las Palmas de Gran Canaria

Facultad de Ciencias del Mar

Departamento de Física

e-mail: alicia.tejera@ulpgc.es

Dr. Pablo Martel Escobar

Universidad de Las Palmas de Gran Canaria

Facultad de Ciencias del Mar

Departamento de Física

e-mail: pablo.martel@ulpgc.es

En Las Palmas de Gran Canaria a 11 de Julio de 2016

Estudiante: Ana del C. Arriola Velásquez

Tutora: Dra. Alicia M. Tejera Cruz

Co-tutor: Dr. Pablo Martel Escobar

INDEX

Abstract.....3

Introduction.....4

Study region.....8

Material and methods.....11

Results and discussion.....16

Conclusions.....21

References.....22

Annex.....26

Personal Assessments.....28

ABSTRACT

In this final degree work an assessment of the impact of environmental radioactivity, mainly on bathers of the most important beach in Las Palmas de Gran Canaria (Las Canteras), has been done. For this purpose, the main radionuclides contained in intertidal superficial sand samples have been measured by using gamma spectrometry analysis. Also alpha activity of the beach water was determined by means of ZnS(Ag) scintillation detector. The radioactivity detected was due to the natural occurring radionuclides ^{226}Ra (^{238}U - series), ^{232}Th and ^{40}K in sand samples with an average activity concentrations of 14.6 ± 1.0 , 17.4 ± 1.0 and 528 ± 24 Bq/kg, respectively. From these values, the outdoor annual effective dose was of 0.047 mSv/y, which is below to the world's average value (0.07 mSv/y). The average gross alpha value for Las Canteras water samples obtained was 0.101 ± 0.003 Bq/L, a similar magnitude to the mean in seawater. Finally, the activity concentrations of ^{40}K in the sand and the gross alpha of the beach water have been suggested as possible tracer of the sedimentary dynamic of the beach and the presence of submarine groundwater discharges, respectively.

1. INTRODUCTION

Radioactivity is around us. It is a process that happens due to the interactions that occurs in the nucleus of the atom between protons and neutrons. Protons push each other away (repulsive electrical force) while nucleons try to hold them together (nuclear force). If these two forces are not in balance the nucleus become unstable or radioactive and decay to another nucleus, stable or also radioactive, emitting the extra energy they have in form of electromagnetic energy and particles (to which we will refer as radiation). There are more than 3000 nucleuses known (nuclides) and only around 100 are stable. This means that most of them are radioactive so they are known as radionuclide (Karam, P.A. and Stein, B.P., 2009).

As described in Pope, J.A., (1989) when an element decay on another (fathers decay on daughters), different kinds of nuclear radiation emissions are produced. These emissions are able to produce ionisation, which is the ability to remove orbital electrons from target atoms, producing a number of ion pairs along its path. Also these emissions have different characteristic of velocity, penetration of matter and mass, depending on the type of particle that is emitted. These would be:

α-emission. If during the decay the particle emitted is a helium nucleus (a particle formed by two protons and two neutrons). This emission is more likely to happen among nucleus of elements with atomic number greater than the lead ($Z=82$). It reduce in 2 the atomic number (Z) of the radionuclide and the mass number (A) is reduced in 4, as it is shown on the next equation:



Father \rightarrow Daughter + Radiation

These α -particles have a high positive charge and a large mass with a small penetration of matter. They have the ability of tear electrons easily from target atoms, leaving behind a dense track of ionisation.

β-emission. In this case we can differentiate two different β -particle emissions. One would be the β^- -emission, in which a neutron is converted in a proton and an electron is released from the nucleus during decay. Normally this decay occurs in radioisotopes with an excess of neutrons. In in this case the mass number (A) stays the same while the atomic number (Z) is increased by 1. Also an antineutrino ($\bar{\nu}$) is released:



The other one would be the β^+ - emission. In this case a proton is converted in a neutron and a positron (the same as an electron but with positive charge) is released. Normally this occur in neutron-deficient radioisotopes. In such decay A stays the same but Z decrease by 1. In addition a neutrino (ν) is released:



The neutrino (ν) and the antineutrino ($\bar{\nu}$) are particles that carry away certain amount of energy and momentum from the decay process but have zero charge and

approximately zero mass. These β -particles have higher penetration of matter than α -particles.

γ -ray emission. Normally these emissions are produced as a photon emitted after another decay process like α - or β -emission that has left the daughter of the initial element in an excited state. This is due to the fact that γ -rays are emitted during transitions from an excited nuclear state to a lower-energy nuclear state in the form of a photon:



Talking about penetration of matter, γ -rays do not have a precise range because they follow very tortuous path, even though they are very penetrating. Also they suffer an exponential drop in intensity as they break through matter. There are three major mechanisms that can produce ionisation by γ -radiation. These would be photoelectric effect (for low photon energy), Compton Effect (for medium photon energy) and pair production (for high photon energy).

Radioactivity is not a man-made phenomenon, contrary to what some might think, although it has both, natural and artificial origins. Some of the natural radionuclides exist since the formation of the earth. The most abundant elements between the former ones are the ${}^{40}\text{K}$ and the radioisotopes from the natural radioactive series of ${}^{238}\text{U}$, ${}^{235}\text{U}$ and ${}^{232}\text{Th}$. Also ${}^{237}\text{Np}$ and its decay products were formed alongside the Earth but, due to its half-life, it was extinct. Nevertheless a small amount of it has been found in small amounts on nature. This ${}^{237}\text{Np}$ is supposed to have been created during the nuclear tests of the XX century. Other elements are produced continuously from the interaction of the cosmic rays with the atmosphere. These rays come from the sun, the stars and the interstellar space and are formed by protons, alfa particles and heavier nucleuses. These particle interact with the nucleuses from the upper atmosphere producing new radioactive species. The production rate of these elements changes with time because the cosmic radiation flux is not uniform. This depends on different factors as the solar activity, human influence on the atmosphere or the changes on the Earth's magnetic fields (Ortega Aramburu, X. and Jorba Bisbal, J., 1996; Azouazi, M., et al., 2000).

The artificial radionuclides are produced mostly by the bombardment of a nucleus with light particles such as protons, neutrons or α -particles. This creates some nuclear reactions that lead to different artificial radioisotopes (Pope 1989). This artificial elements can be released to the environment by different means and from different origins. Some of them have been released from the nuclear weapon testing during the middle of XX century, from nuclear weapons production or from nuclear accidents on the industry. Others are released from the general used of radioactive materials on medicine, non-nuclear industries producing Naturally-Occurring Radioactive Materials (NORM industry), research and space exploration (Livingston, H.D., 2004).

Natural radioisotopes have different distribution in earth crust and in the oceans. In table 1 the worldwide activity concentration value of radioisotopes ${}^{226}\text{Ra}$ (a representative isotope of the ${}^{238}\text{U}$ decay series), ${}^{232}\text{Th}$ and ${}^{40}\text{K}$ is shown. This values

correspond to the mean value concentration of natural radioisotopes on the earth crust and are given on Bq/kg (1Bq= 1 radioactive decay per second).

Location	²²⁶ Ra	⁴⁰ K	²³² Th
Worldwide	32	420	45

Table 1. Mean activity concentration of natural radionuclides on earth crust in Bq/kg (UNSCEAR 2000).

In addition to the difference with the earth crust, radionuclide concentration in the ocean varies from one nuclide to another. In table 2 it is shown the main different radionuclides that can be found on seawater. Also appears their concentration and activity in mBq/L for seawater.

Radionuclide	Concentration (g/L) (mBq/L)	
³ H	3.2x10 ⁻¹⁸	1.11
¹⁴ C	3.1x10 ⁻¹⁴	22.2
⁴⁰ K	4.5x10 ⁻⁵	11840
⁸⁷ Rb	3.4x10 ⁻⁵	107.3
²²⁶ Ra	8.0x10 ⁻¹⁴	2.96
U(²³⁸ U & ²³⁴ U & ²³⁵ U)	3.3x10 ⁻⁶	81.4
²³² Th	2.0x10 ⁻⁸	0.074

Table 2. Concentrations and activities of radionuclides in seawater. Modified from Garzón Ruiperez, L., (1979).

In general, it is worth noting that the concentrations of ²³⁸U, ²³²Th and its daughters are smaller in seawater than in earth's crust. Depending on the environmental conditions U can be found in different forms, so that sometimes uranium ores can be insoluble and they are deposited on sediments. Also the relation Th/U is 6*10⁻⁴, while in continents it has a value of 2-3. This shows that seawater is impoverished on Th in contrast to continents. This relation can give an idea of the high stability that Th ores present against U ones, since all of them are contributed by continental water discharges. Another radionuclide that can vary depending on the conditions is the ²²⁶Ra. Being a daughter from ²³⁸U, the concentration of ²²⁶Ra could be calculated but the result would be higher than the one indicated on table 2. This means that part of the ²²⁶Ra is deposited on sediments. Also some marine organism are able to concentrate this radionuclide. As a result, the presence or absence of this organisms can change noticeably the presence of ²²⁶Ra in seawater. In addition this element also has a smaller presence in seawater than in continents. Finally the nuclide that contributes more, by far, to the total activity of seawater is the ⁴⁰K. This radionuclide represent the 98% of the total activity (Garzón Ruiperez, L., 1979).

Different activity concentrations in marine sediments from different parts of the world are shown in table 3. As it can be observed, the average concentration for natural radionuclides is different from one place to another. These variations give and idea that the presence of radionuclides varies depending on the composition of the sample that is analysed.

Location	²²⁶ Ra		⁴⁰ K		²³² Th		Reference
	Range	Mean	Range	Mean	Range	Mean	
Rizhao beaches (China)	8-17	12	883-1314	1079	8-25	15	Lu, X. & Zhang, X., 2008
Beaches of Aegean sea (Turkey)	79-1885	290	687-1421	1160	97-4360	532	Örgün, Y., et al., 2007
Sediments of Cadiz Bay (Spain)	3-41	13	105-1342	451	3-73	19	Casas-Ruiz, M., et al., 2012
Montenegrin coast (Yugoslavia)	2-16	8	16-263	150	1-12	7	Vukotic, P., et al., 1998
Rio de Janeiro coast (Brazil)	5-286	33	32-888	253	7-963	95	Veiga, R., et al., 2006

Table 3. Activity concentrations (Bq/kg) of natural radionuclides in different parts of the world.

According to Pope, J.A., (1989), for measuring all this radioactivity and its effect on the matter different parameters are proposed. One would be the absorbed dose:

$$D = \frac{E}{m} \quad (5)$$

where E is the mean energy imparted by ionising radiation to a volume of mass m. In other words, this parameter gives information about the radiation absorbed by any kind of matter. Its unit is J/kg, also known as Grey (Gy). But the biological effects on matter not only depend on absorbed dose. Depending on the type of ionizing particle the biological damage will be important, even if the energy absorbed is the same in one case and another. To measure the effectiveness of a concrete ionizing particle in producing biological damage, the dimensionless quality factor (Q) is used (1-2 for X, γ - and β -radiation, 5 for low neutron, 10 for fast neutrons, protons and α -particles and 5 for heavy recoil nuclei).

Also it depends on the distribution of absorbed dose in space and time. This factor would be grouped on the N parameter. For external sources N is taken as 1 but for ingested radiation material can change. With the absorbed dose, Q and N factor dose equivalent (H) can be calculated:

$$H = D \times Q \times N \quad (6)$$

Dose equivalent thus explains the relative radiation risk of a particular radiation. Its units would be J/kg, as the absorbed dose. To distinguish one from another, Sievert unit (Sv) is assigned to dose equivalent.

In figure 1 the main sources of annual doses absorbed by a person are shown. It appears an element called Radon. This is a radioactive gas that comes mainly from the radioactive series of ²³⁸U, in form of ²²²Rn and on smaller magnitude from the ²³²Th series, in form of ²²⁰Rn (Bonotto, D.M., 2014). As it can be appreciated radon radiation represents almost half of the natural radiation received.

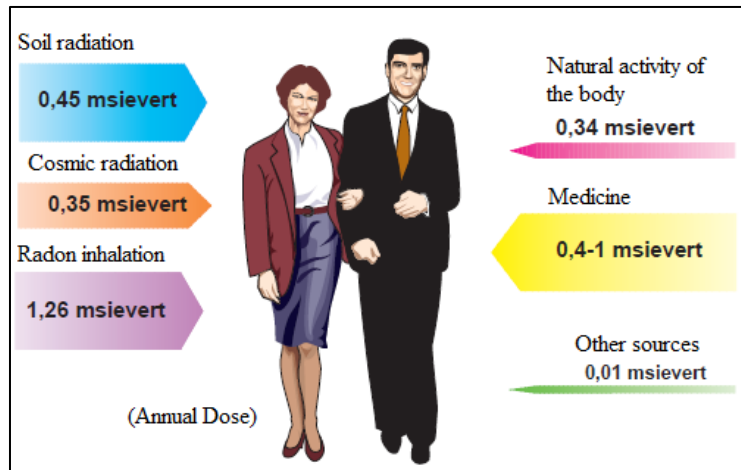


Figure 1. Annual Dose received by a person and its different sources.
Modified from CSN, (2004).

The aim of this work is to give a radiological characterization of the most important beaches of Gran Canaria, Las Canteras. For this purpose γ -emissions and α -emissions will be measured in order to establish a baseline of natural and artificial radioactivity present on the area of study, as well as to evaluate the possible radiological hazards related to it. This assessment of the impact of environmental radioactivity, mainly on the bathers, will be obtained by analysing of intertidal superficial sand and water beach samples. After describing the study region, the methodology development in this work is presented. Main results and conclusions of this final degree work are exposed in sections 4 and 5, where, in addition to the radiological impact assessment, we point the possibility of the use of certain measures obtained in this work as tracers of different environmental processes in the beach. In the last section the references used in present study are listed. Finally, an annex, including the method followed to determine an important quantity for alpha radioactivity analysis of the water samples, which was carried out during the traineeship, is added.

2. STUDY REGION

The Canary Islands are located in the NE of the central Atlantic Ocean, between $27^{\circ} 37' - 29^{\circ} 25' N$ and $13^{\circ} 20' - 18^{\circ} 10' W$. The island of Gran Canaria is situated in a relatively central position and its surface is of 1532 km^2 . It is a volcanic island, originated by a "hot spot" inside the oceanic crust associated to the passive continental margin of the African plate (Figure 2). The volcanic materials emitted during its creation were stacked during different eruptive phases and inactivity periods that happened during the last 14.5 million years. The current morphology of the island was created after three important magmatic cycles and erosive and sedimentary processes in-between the magmatic cycles. These periods of magmatic activity are known as "Ciclo I or Ciclo Antiguo" during the Miocene. The second one is the "Ciclo II or Ciclo del Roque Nublo" starting at the Early Pliocene. The last one is the "Ciclo III or Ciclo Reciente" that has not finished yet (Pérez-Torrado, F.J., 1992).

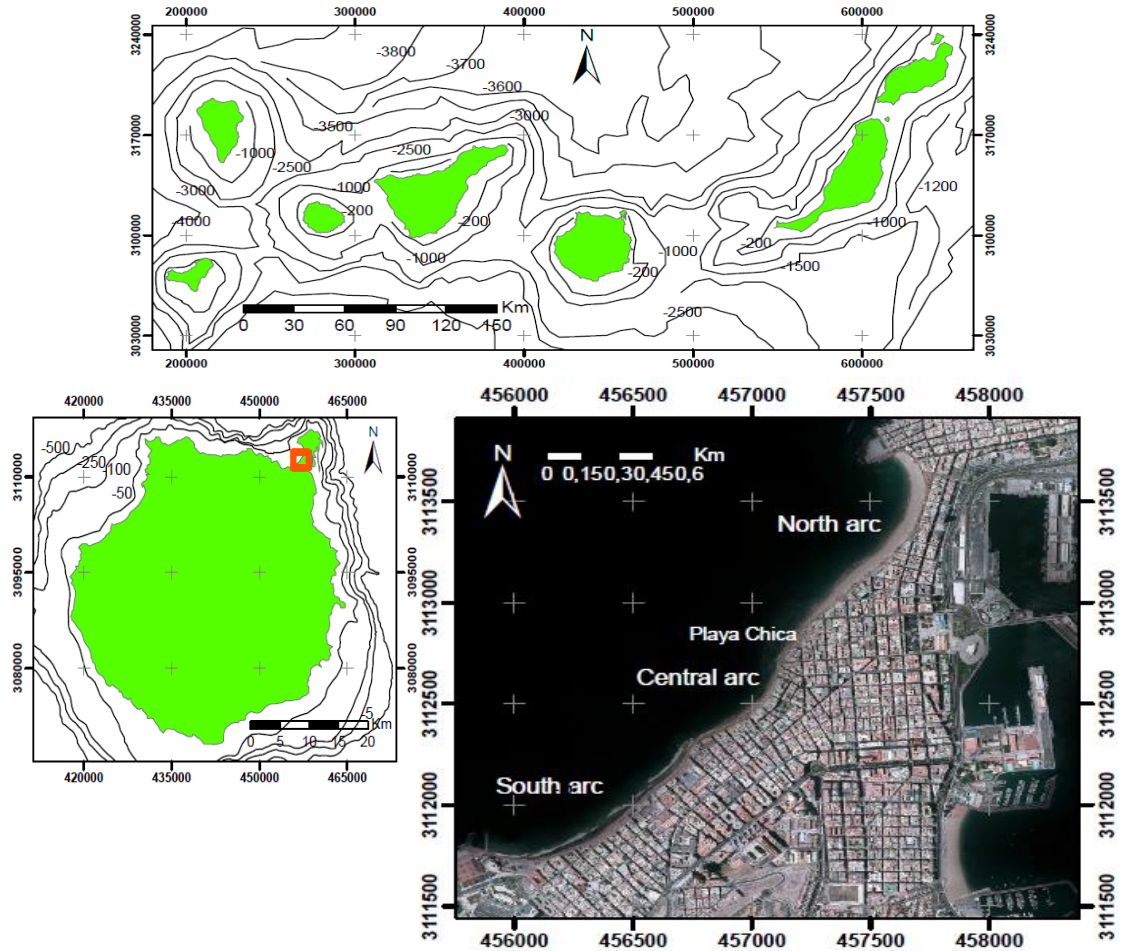


Figure 2. Location and division of Las Canteras beach.

This study is focused on one of the most important beaches of the city of Las Palmas de Gran Canaria, Las Canteras, located in the north coast of the island. According to Déniz-González, I. and Mangas, J., (2012), the geologic elements on the area of Las Palmas de Gran Canaria will englobe six different kinds of rocks that belong to different time periods from the Miocene to the Holocene. Nevertheless, in the study area the sedimentary deposits that emerge are the ones from the Detrital Formation of Las Palmas during the Miocene (Pérez-Torrado, F.J., et al., 2000).

Las Canteras beach is an approximately 3 km long sandy beach. It is delimited by La Isleta itmus in the north and a breakwater in the south. This beach can be divided in three different sectors. The first one is the northern arch. This goes from La Puntilla to approximately Tomás Miller Street and it has 950 m length. The second one is the central arch that goes from Tomás Miller Street to Gravina Street. It has 900 m length. The last one is the southern arch. This has 1000 m length and it goes from Gravina Street to La Ballena ravine (Alonso, I., 1993). During the year, the water temperature range between 18 and 24°C, being higher in summer than in winter. At high tide periods tide currents are to NE while during the low tide periods they are SW. The wind direction is mainly NE, NNE and ENE due to the trade winds. During spring tides the tidal range is greater than 2.5 m and during neap tides is approximately of 1 m. The mean wave approaching direction is north and during big storms comes from the northwest. The average significant wave height is 1.42 ± 0.6 m, being able to reach 4 m

on winter (Casanova, M., 2015). The northern part of the beach is well protected by a natural offshore rocky bar. This bar has a length of 200-250 m. It has a height similar to the mean sea level of the zone. Because of that this part of the beach is less exposed to waves than the one in the southern arch. Also the presence of the beachrock influence causes differences between the sedimentary dynamic on the different parts of the beach (Alonso, I., 2005).

The sediments that compose the sand of the beach are provided by the Isleta isthmus, La Ballena Ravine and the beachrock that can be found in the different parts of the beach. Also they come from submerged sandbars that are located between the bathymetric curve of 50 m and all the beachfront. The sand all across the beach can be considered medium and fine sands, with a size around 0.25 mm of diameter (Alonso, I., 1993). As first indicated in Alonso, I. and Pérez-Torrado, F.J., (1992) and then in Alonso, I., (1993), calcimetry analysis made in these studies show that the lower values of calcareous matter are located in the part of La Cicer in the southern arch. This is due to the absence of a substrate in this part of the beach where life could develop. They suggest too that some of the organic matter comes from the Confital beach in the Isleta isthmus. These materials would be deposited in the northern arch, the part of the beach that is nearest to El Confital. Petrographic studies carried on also support that in the southern arch the composition of sand is bigger in minerals than in organic matter. In addition the densest minerals that are contributed by La Ballena ravine stay in the southern arch while the rest of minerals and organic matter are redistributed along the beach.

The sedimentary deposits on the beach belong to the Detrital Formation of Las Palmas. They emerge on the area between Playa Chica and Churruca Street, in the central and northern arch. Also they appear in the different fragments of the offshore rocky bar that is present on the north sector of the beach. These deposits have five well defined stratigraphic units that reflect the different sub-environments that coexist on the beach. The first unit, the second and the fourth are calcarenites. Their principal components are Rhodophyta algae, pieces of mollusks, bivalves and lithoclasts. The third unit is a silt with a high composition of gastropods. The last unit, unit five, is mainly composed by some boulders of phonolitic and basaltic nature (Pérez-Torrado, F.J., et al., 2000).

Following the work of Alonso, I., (1993) and Alonso, I. and Vilas, F., (1996), we can describe the sedimentary balance of Las Canteras beach. This beach presents a seasonal variability with two different periods, erosion and accumulation. On the one hand, erosion period normally occurs during storm events so it is logic to expect it to occur during winter. On the other hand accumulation period normally happens during summer. Even though this is the expected behavior of the sedimentary balance, it is important to mention that any big storm can cause an erosion period. Also the beach have a different behavior in the different parts. During erosion periods the southern arch losses a big amount of sediment that is transported to the northern arch. During accumulation periods the sand of the submerged sandbars is transported to the beach so the amount of sediment on the beach increase forming berms. At some point, because the southern arch is not protected by de offshore rocky bar, the higher part of the sedimentary input is located on the northern arch.

3.- MATERIAL AND METHODS

3.1.-Sample collection

A total of thirty six sand and water samples, 30 and 6 respectively, were collected along Las Canteras beach. Ten points were selected in each campaign to sampling, four located on the south arch, one in the central arch, another one in Playa Chica and the last four in the north arch (figure 3).

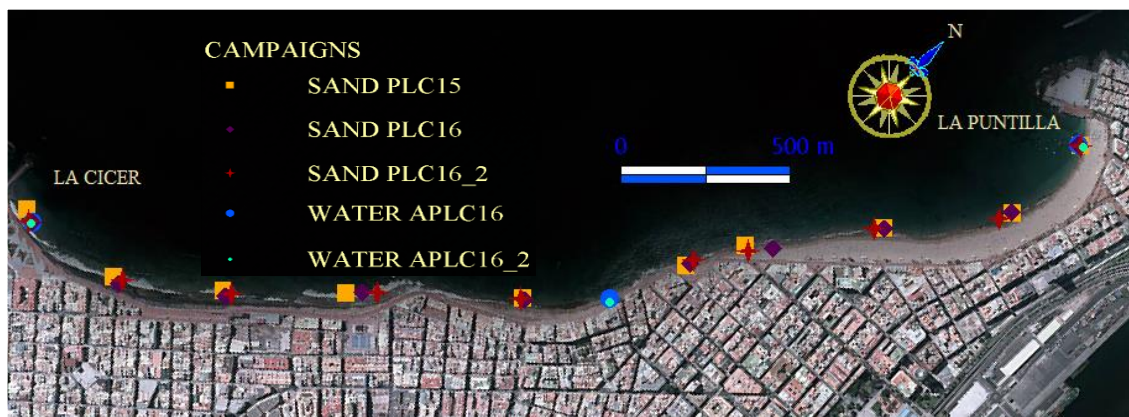


Figure 3. Location of the sampling points for radionuclides analysis.

In order to take samples from an erosion and recovery periods, the collection of sand took place during three campaigns, the first one in middle of October 2015, the second one at the end of January 2016 and the third one at the beginning of May 2016. During the second campaign three samples of water were collected. One was taken from La Cicer, another one in La Puntilla and the third one was taken in Peña La Vieja, near Playa Chica. A second collection of water was made in middle April 2016, at the same points as water was collected on January 2016. The table 4 shows the name of sample (PLC for sand APLC for water), place of collection, date and coordinates of collection.

Muestra	Playa	Fecha cierre	Coordenadas	
			X-UTM	Y-UTM
PLC15_1	Southern arch	21/10/2015	455957	3111778
PLC15_2	Southern arch	21/10/2015	456216	3111814
PLC15_3	Southern arch	21/10/2015	456426	3111975
PLC15_4	Southern arch	21/10/2015	456638	3112179
PLC15_5	Central arch	21/10/2015	456945	3112470
PLC15_6	Playa chica	21/10/2015	457166	3112801
PLC15_7	Northern arch	21/10/2015	457233	3112934
PLC15_8	Northern arch	21/10/2015	457438	3113197
PLC15_9	Northern arch	21/10/2015	457630	3113441
PLC15_10	Northern arch	21/10/2015	457633	3113669
PLC16_1	Southern arch	29/01/2016	455988	3111766
PLC16_2	Southern arch	29/01/2016	456236	3111809
PLC16_3	Southern arch	29/01/2016	456436	3111971
PLC16_4	Southern arch	29/01/2016	456663	3112207
PLC16_5	Central arch	29/01/2016	456949	3112471
PLC16_6	Playa Chica	29/01/2016	457167	3112811
PLC16_7	Northern arch	29/01/2016	457283	3112975
PLC16_8	Northern arch	29/01/2016	457439	3113198

PLC16_9	Northern arch	29/01/2016	457627	3113440
PLC16_10	Northern arch	29/01/2016	457628	3113666
PLC16_2.1	Southern arch	05/05/2016	455978	3111764
PLC16_2.2	Southern arch	05/05/2016	456236	3111825
PLC16_2.3	Southern arch	05/05/2016	456443	3111984
PLC16_2.4	Southern arch	05/05/2016	456688	3112233
PLC16_2.5	Central arch	05/05/2016	456940	3112466
PLC16_2.6	Playa Chica	05/05/2016	457168	311282
PLC16_2.7	Northern arch	05/05/2016	457247	3112930
PLC16_2.8	Northern arch	05/05/2016	457423	3113180
PLC16_2.9	Northern arch	05/05/2016	457616	3113410
PLC16_2.10	Northern arch	05/05/2016	457634	3113667
APLC2016_1	Northern arch	29/01/2016	455988	3111766
APLC2016_2	Peña La Vieja	29/01/2016	457091	3112617
APLC2016_3	Southern arch	29/01/2016	457628	3113666
APLC2016_2.1	Northern arch	14/07/2016	455987	3111764
APLC2016_2.2	Peña La Vieja	14/07/2016	457098	3112611
APLC2016_2.3	Southern arch	14/07/2016	457639	3113668

Table 4. Samples information.

Sand samples were collected in the intertidal zone during low tide. A square of 1 m² was drawn on the sand and, after mix them in situ, samples were taken from the superficial sand (figure 4). Water was taken from around 30-40cm of depth, except in La Cicer. There, to avoid turbulences of the water, the sample was taken from around 50 cm of depth. Approximately 1L of water were taken in each point.



Figure 4. Delimitation of the area for sand sample.

3.2.- Sample preparation

a) Sand samples

Sand samples were taken to the laboratory and were oven dried at 80°C for 48 hours. After this period samples were taken out of the oven and screened through a 1 mm mesh size sieve. Finally they were kept inside PVC-trunk conical containers sealed with aluminum strips (figure 5). Aluminum was used due to their impermeability to

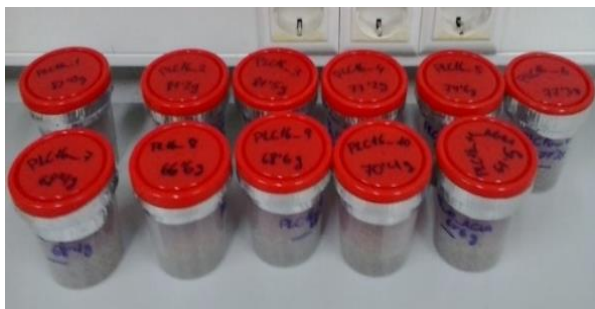


Figure 5. Sand Samples in PVC-trunk conical containers.

avoid the bacterial growth before its preparation for measurement. The coprecipitation method was used to determine the gross alpha activity (Suárez-Navarro, J.A., et al., 2002; Llauradó, M. et al., 2006; Montaña M., et al., 2013).

First, 0.5 L of water sample was taken to neutral pH with NH_4OH . After that the sample was acidified with H_2SO_4 and put on a heating plate and was taken to boiling point for 10 minutes in order to eliminate the radon and CO_2 . Subsequently, temperature was decreased until it arrived to 50 °C to obtain a radium precipitate. At this new temperature, 1 ml of barium carrier was added to drag the radium dissolved and the dissolution was kept between 45 and 50 °C during thirty minutes. Then, 1 ml of iron carrier was added with 1 ml of bromocresol purple as an indicator. Some drops of NH_4OH were added until the indicator turned purple to control the pH. This was made in order to establish a pH control of the sample. Afterwards, the sample was in stirring during 30 minutes. Then it was cooled in cold water, at approximately 0°C, during 15 minutes. In this way radium, polonium and actinides are coprecipitated. After, the dissolution was filtered using a 0.45µm filter and vacuum system (Figure 6). Before we used it, the filter was put into a structure formed by a steel planchette and a steel ring. This structure was dried during an hour inside an oven at 105 °C and then was kept inside a desiccator to protect it from the wet. In order to know the exact mass of the precipitate the structure was weighed three times in a precision scale. One before getting it into the oven, another one after taking it out of the oven and the last one 15 minutes after putting it inside the desiccator. After the dissolution was filtered, the same procedure was taken with the filter that contained the precipitate. Finally, sample was kept inside the desiccator for two days before its measurement. This is because during sample preparation, and just after the filtering steps, ^{222}Rn from the air is trapped in the precipitate and produces the alpha emitter ^{218}Po and ^{214}Po increasing and varying the alpha contribution in the sample (Montaña, M., et al., 2013).



Figure 6. Vacuum system used to filter the water sample.

3.3.- Radiological analysis

The determination of radioisotopes on sand samples by gamma-ray spectrometry analysis was carried out using a Gemanio Canberra XtRa coaxial detector, model GX3518 7500 SL (figure 7.a) (Arnedo, M.A., et al., 2013). This has a 35% of relating efficiency and a nominal FWHM of 1.1 keV at 88 keV.

The measurement of gross alpha in water samples was made in a ZnS(Ag) scintillation alpha-detector (figure 7.b). It consists on a flat ZnS (Ag), which is located above the sample and is used for counting and to determinate the gross alpha, and a Canberra photomultiplier tube base/preamplifier, model 2007P.

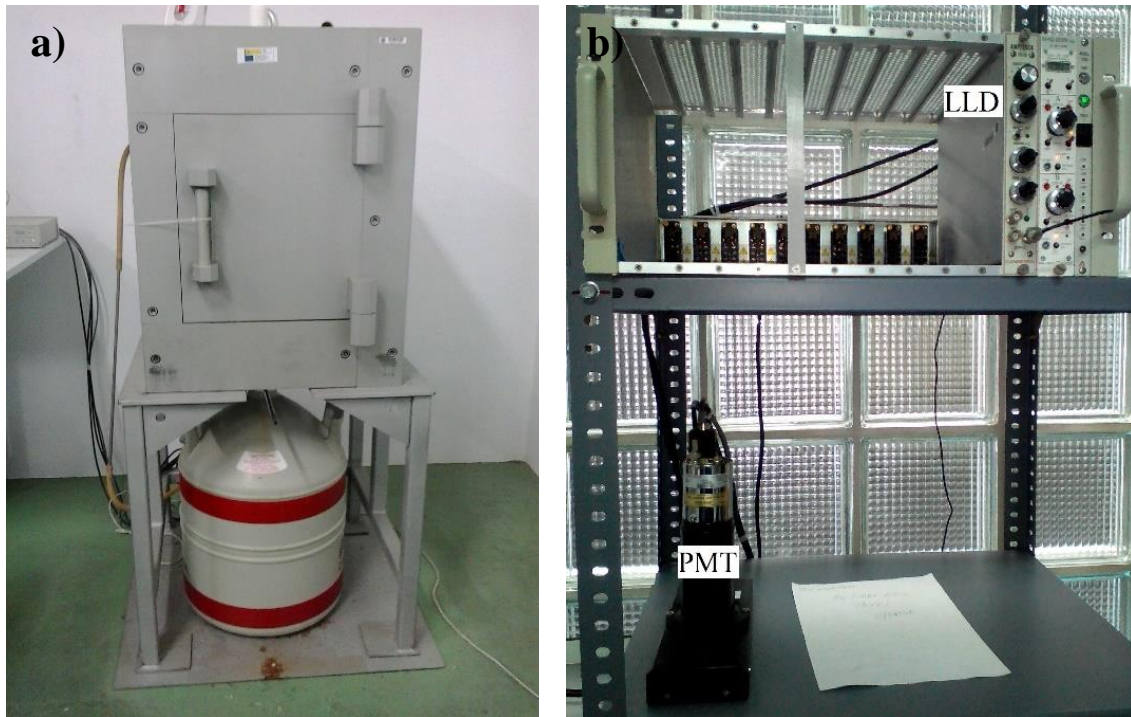


Figure 7. a) Gamma-Ray detector. b) Gross alpha detector.

3.4.- Activity calculation

Activity of sand samples can be calculated with the next equation (Arnedo, 2014):

$$A = \frac{cps}{\varepsilon \times P(E) \times m} \quad (7)$$

where cps is the net count rate, P(E) is the emission probability of each gamma-ray, ε correspond to the efficiency coefficient, m is the mass of dry sample in kg. The uncertainty associated to this activity can be calculated with the equation (Arnedo, M.A., 2014):

$$U(A) = A \sqrt{\left(\frac{U(cps)}{cps}\right)^2 + \left(\frac{U(\varepsilon)}{\varepsilon}\right)^2 + \left(\frac{U(P(E))}{P(E)}\right)^2 + \left(\frac{U(m)}{m}\right)^2} \quad (8)$$

The activity concentration measurement for the radionuclides of interest were realized with the following methodology:

- Radium (^{226}Ra): This was taken as a representative of the ^{238}U decay series. An indirect measurement was made based on the activity concentration value of ^{214}Pb found by analysing the gamma-ray photopeak with energy 351.9 keV.
- Thorium (^{232}Th): This was calculated from the activity concentration values of ^{212}Pb and ^{228}Ac obtained following the ISO 11929.
- Potassium ^{40}K : This was obtained directly from the analysis of gamma-ray photopeak with energy 1460.8 keV.

For water samples the gross alpha activity index was calculated following the equation (Llauradó, M., et al., 2006):

$$A = \frac{cpm_{\text{alfa}} - cpmb_{\text{alfa}}}{60 \times E \times F_i \times V} \quad (9)$$

where cpm_{alfa} is the alpha counting rate of the sample in counts per minute, $cpmb_{\text{alfa}}$ is the alpha counting rate of the reference sample also in counts per minute. E is the efficiency of the used detector and F_i is the self-absorption factor. This parameter is calculated from an absorption curve that is created with standard of ^{241}Am as it is described in Annex. V corresponds to the volume of the sample, in this case 0.5 L.

There is an error associated to this activity that is known as count uncertainty in the determination of gross alpha activity index. For calculate this uncertainty the following equation is used:

$$u(A) = \frac{2}{60 \times E \times F_i \times V} \sqrt{\frac{cpm_{\text{alfa}}}{t(m)} + \frac{cpmb_{\text{alfa}}}{t(b)}} \quad (10)$$

In this case cpm_{alfa} , $cpmb_{\text{alfa}}$, E, F_i and V are the same parameters as in the calculation of gross alpha activity. The measurement time is represented by $t(m)$ and $t(b)$, being the measurement time of the sample and the blank respectively.

The minimum detectable activity for gross alpha activity index, for a confidence level of 95%, was also calculated with the expression:

$$AMD = \frac{3.29 \sqrt{\frac{cpm_{\text{alfa}}}{t(m)} + \frac{cpmb_{\text{alfa}}}{t(b)}} + 2.7 \times \left(\frac{1}{t(m)} + \frac{1}{t(b)} \right)}{60 \times E \times F_i \times V} \quad (11)$$

where cpm_{alfa} is the alpha counting rate of the sample in counts per minute. The alpha counting rate of the reference sample is represented by $cpmb_{\text{alfa}}$ and its unit are counts per minute. E is the efficiency of the detector used unit, F_i is the self-absorption factor and V is the volume of the sample in L. The measurement time is represented by $t(m)$ and $t(b)$, being the measurement time of the sample and the blank respectively.

4.- RESULTS AND DISCUSSION

4.1.- Activity concentration distribution of ^{226}Ra , ^{232}Th and ^{40}K

The activity concentration ^{226}Ra , ^{232}Th and ^{40}K for each sample is represented in figure 8. Table 5 shows the average activity concentration of these radioisotopes on each part of the beach is shown. The mean value of points 1, 2, 3 and 4 corresponds to the southern arch, points 5 and 6 to the central arch and points 7, 8, 9 and 10 are used for the northern arch. For each location three different values are presented corresponding to the three different campaigns that were carried out.

Activity concentration of ^{226}Ra ranges from 8.4 to 18.5 Bq/kg (mean value 15.4 ± 1.0 Bq/kg), from 8.8 to 19.0 Bq/kg (mean value 14.2 ± 1.0 Bq/kg) and from 6.1 to 20.68 Bq/kg (mean value 14.1 ± 0.9 Bq/kg) in the first, second and third campaign, respectively.

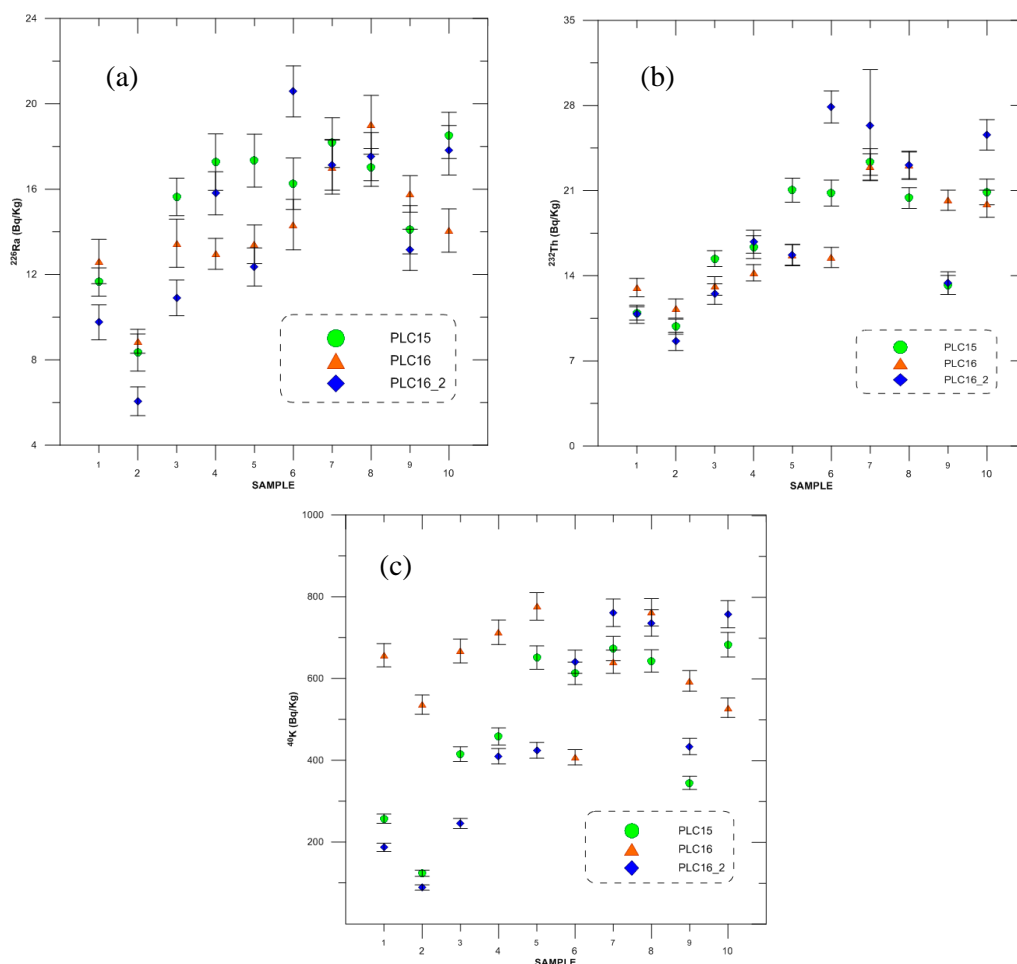


Figure 8. Comparison of activity concentration (Bq/kg) of ^{226}Ra (a), ^{232}Th (b) and ^{40}K (c) on each sample in each campaign.

Activity concentration of ^{232}Th ranges from 9.8 to 23.4 Bq/kg (mean value 17.2 ± 0.9 Bq/kg), from 11.3 to 23.1 Bq/kg (mean value 16.9 ± 0.9 Bq/kg) and from 8.6 to 27.9 Bq/kg (mean value 18.1 ± 1.3 Bq/kg) in the first, second and third campaign, respectively.

Campaign	Area	^{226}Ra	^{232}Th	^{40}K
PLC15	Southern arch	13.2±0.9	13.1±0.7	313± 14
PLC15	Central arch	16.8±1.2	20.9±1.0	632± 28
PLC15	Northern arch	16.8±1.1	19.7±1.0	591± 26
PLC16	Southern arch	12.0±0.9	12.9±0.7	643± 28
PLC16	Central arch	13.9±1.0	15.6±0.8	592± 26
PLC16	Northern arch	16.5±1.1	21.5±1.0	631± 28
PLC16_2	Southern arch	10.6±0.8	12.2±0.8	237± 12
PLC16_2	Central arch	16.5±1.0	21.8±1.1	579± 26
PLC16_2	Northern arch	16.4±1.1	22.1±2.0	646± 29

Table 5. Average activity concentration of ^{226}Ra , ^{232}Th and ^{40}K in Bq/kg in the different zone of Las Canteras beach.

Finally the activity concentration of ^{40}K ranges from 124 to 683 Bq/kg (mean value 486±22 Bq/kg), from 407 to 776 Bq/kg (mean value 628±27 Bq/kg), and from 90 to 762 Bq/kg (mean value 470±21 Bq/kg), in the first, second and third campaign, respectively.

In all three cases the third campaign is the one with the largest range of activity concentration. The activity concentrations of ^{226}Ra in La Cícer (southern arch) are slightly lower than those found in areas of Playa Chica (central arch) and La Puntilla (northern arch). This behaviour also presents the ^{232}Th . Furthermore, the three campaigns show no significant variations in the mean values of activity concentration for both ^{226}Ra and ^{232}Th along the beach. The $^{232}\text{Th}/^{238}\text{U}$ ratio represented by the $^{232}\text{Th}/^{226}\text{Ra}$ was calculated and they are maintained throughout the beach with a coverage factor of 2. The ^{235}U has not been detected in any sample.

Instead, the average value of activity concentration of ^{40}K show remarkable variations along the beach and on the different time periods. In 2015 the southern arch had almost half the activity of the rest of the beach while in January 2016 there is a significant increase of activity, reaching in the southern arch the values of the central and northern arch. In May 2016 the data show that the values of the southern arch have significant decreasing reaching lower values than on the first campaign. This changes in the activity concentration of ^{40}K might indicate some change on sand composition of the area of the southern arch in the second campaign that made it similar to the rest of the beach.

Anthropogenic radioactivity (artificial radionuclides) has not been detected; more specifically ^{137}Cs . Global fallout is associated with the testing of nuclear weapons, and also as a result of the accident of the nuclear power plant in Chernobyl (Aarkrog, A., et al., 1999; Livingston, H.D., 2004).

4.2.- Analysis of $^{210}\text{Pb}_{\text{excess}}$

^{210}Pb is a radioisotope that comes from the ^{238}U decay series. It is originated after the decay of ^{226}Ra that produces ^{222}Rn , a short-lived gas that then end up producing ^{210}Pb that is in equilibrium with the parent ^{226}Ra . As ^{222}Rn is a gas, part of it diffuses upward into the atmosphere and once it arrives there it rapidly decays into ^{210}Pb that is deposited as fallout. Atmospheric fallout, like rain snow and dry deposition, also help to deposit ^{210}Pb on the ground. This ^{210}Pb deposited is known as unsupported or

excess ^{210}Pb (Mabit, L., et al, 2008; Hülse, P. and Bentley Sr, S.J., 2012). This $^{210}\text{Pb}_{\text{ex}}$ is obtained by the difference between the activity concentration of ^{210}Pb and the activity concentration of ^{226}Ra , which is assumed in secular equilibrium, measured on the detector (Sanchez-Cabeza, J.A., et al, 2012; Szmytkiewicz, A. and Zalewska, T., 2014).

The unsupported lead activity is represented in figure 9 for each sample and for each campaign. The average values for each part of the beach and campaign are shown in table 6.

Activity concentration of $^{210}\text{Pb}_{\text{ex}}$ ranges from 18.5 to 51.2 Bq/kg (mean value 34.4 ± 5.8), from 12.6 to 36.8 Bq/kg (mean value 27.1 ± 6.2) and from 16.2 to 46.4 Bq/kg (mean value 29.4 ± 6.8) for the first, second and third campaign, respectively. While the ranges vary slightly from one campaign to another, the average values of the different parts of the beach show that there is no variation or along the beach or on the different campaigns.

These similar values along the beach on the three different campaigns could indicate the idea that the fallout is the factor which determines the constant deposition of $^{210}\text{Pb}_{\text{ex}}$ through time (Mabit, L., et al, 2008) but, since there are not previous works on this subject in the study area and the samples are only superficial sand, a further study should be done.

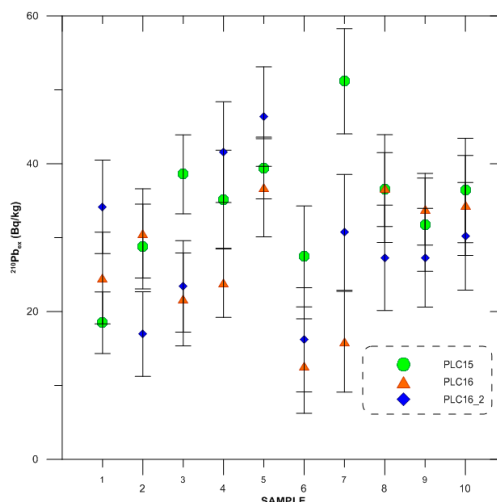


Figure 9. Comparison of activity concentration (Bq/kg) of $^{210}\text{Pb}_{\text{ex}}$ on each sampling point in each campaign.

Campaign	Area	$^{210}\text{Pb}_{\text{ex}}$
PLC15	Southern arch	30.3 ± 5.5
PLC15	Central arch	33.4 ± 5.5
PLC15	Northern arch	36.7 ± 6.5
PLC16	Southern arch	25.2 ± 5.8
PLC16	Central arch	24.7 ± 6.5
PLC16	Northern arch	30.2 ± 6.4
PLC16_2	Southern arch	29.0 ± 6.3
PLC16_2	Central arch	31.3 ± 6.9
PLC16_2	Northern arch	28.9 ± 7.2

Table 6. Average activity concentration of $^{210}\text{Pb}_{\text{ex}}$ (Bq/kg) in the different parts of Las Canteras Beach.

4.3.- Radiological risks assessment

For measure the radiological risk assessment the external dose rate, the outdoor annual effective dose (H), the external hazard index (H_{ex}) and the radium equivalent ($R_{\text{a}_{\text{eq}}}$) were calculated. These were determined for each part of the beach. The results are shown in table 7.

Area	D (nGy/h)	H (mSv/y)	H _{ex}	Ra _{eq} (Bq/kg)
Southern arch	29.8±1.6	0.037±0.002	0.17±0.01	60.7±3.3
Central arch	43.4±2.2	0.053±0.003	0.24±0.01	88.6±4.5
Northern arch	46.8±2.5	0.057±0.003	0.26±0.01	95.4±5.1

Table 7. The external gamma dose rate, outdoor annual effective dose rate, the radium equivalent and the external hazard index for the different parts of Las Canteras beach.

The external gamma dose rate (D) due to natural radioisotopes at 1 m above the ground level was calculated following the equation (Arnedo, M.A., et al., 2013):

$$D = 0.462A_{Ra} + 0.0417A_K + 0.604A_{Th} \quad (12)$$

where A_{Ra} , A_K and A_{Th} are the activity concentrations of ^{226}Ra , ^{40}K and ^{262}Th in Bq/kg. The units of the external dose rate are nGy/h. The highest values of external dose rates were found on the central and northern arch with a value of 43.4 ± 2.2 and 46.8 ± 2.5 nGy/h respectively. These values are lower than the Spain mean which is 76 nGy/h but still are in the range of Spain gamma dose rate that goes from 40 to 120 nGy/h (UNSCEAR 2000). The value of the southern arch is smaller than the Spain mean with a value of 29.8 ± 1.6 nGy/h. Even though these values are smaller than the values found on Spain, comparing with the work of Arnedo, M.A., et al, (2013) the values are near to the Gran Canaria mean value (43.9 ± 2.8 nGy/h). In the case of the southern arch the value also is similar to the value found in that work on Las Canteras beach (31.5 ± 2.4 nGy/h).

The outdoor annual effective dose is another type of absorbed dose that is calculated following the equation (Arnedo, M.A., et al., 2013):

$$H = D \times F \times T \times O \times 10^{-6} \quad (13)$$

where D is the external dose rate given in nGy/h, F is the absorbed to the effective dose conversion factor (0.7 Sv per Gy), T is h per y^{-1} (8760), O is the occupancy factor (0.2) and 10^{-6} is the nano to milli conversion factor. The outdoor annual effective dose is given in mSv/y. Again the values of the central and the northern arch (0.053 ± 0.003 and 0.057 ± 0.003 mSv/y respectively) are higher than the value of the southern arch (0.037 ± 0.002 mSv/y). All values on Las Canteras beach are smaller than the world's average which is 0.07 mSv/y (UNSCEAR 2000). The value found in the southern arch is similar to the value of 0.038 ± 0.003 mSv/y found for Las Canteras beach in Arnedo, M.A., et al, (2013).

Another parameter that is useful to measure the radiological risks of an area is the external hazard index (H_{ex}) that is calculated with the equation (Elisha, J.J., et al., 2013):

$$H_{ex} = \frac{A_{Ra}}{370} + \frac{A_{Th}}{259} + \frac{A_K}{4810} \quad (14)$$

where A_{Ra} , A_K and A_{Th} are the activity concentrations of ^{226}Ra , ^{40}K and ^{262}Th in Bq/kg. In this case the value of H_{ex} for each part of the beach must be less than 1 in order to keep the radiation risks insignificant. In all the three areas of the beach the value was under the unit with a maximum value of 0.26 ± 0.01 on the northern arch and a minimum

value on the southern arch of 0.17 ± 0.01 . The value of the southern arch is also similar to the value of 0.18 ± 0.01 found in Arnedo, M. A., et al, (2013) for Las Canteras beach.

If the sand were to be used as building material the last parameter that should be calculated is the Radium equivalent activity (Ra_{eq}). This allows the comparison of the activity concentration of samples with different amounts of ^{226}Ra , ^{232}Th and ^{40}K . It is calculated with the equation (Elisha, J.J., et al., 2013):

$$Ra_{eq} = A_{Ra} + 1.43A_{Th} + 0.077A_K \quad (15)$$

where A_{Ra} , A_K and A_{Th} are the activity concentrations of ^{226}Ra , ^{40}K and ^{232}Th in Bq/kg. The highest value was found on the northern arch, with a value of 95.4 ± 5.1 Bq/kg, and the smallest value was found on the southern arch, 60.7 ± 3.3 Bq/kg. The average value found in Las Canteras beach (81.6 ± 4.3) is similar to the overall average value of Gran Canaria (91.3 ± 5.9) given in the work of Arnedo, M.A., et al., (2013), and is also less the safe limit value of 370 Bq/kg. Instead, the value for Las Canteras beach found in that work (64.9 ± 5.1) was smaller than the mean value found in this work but similar to the value of the southern arch.

4.4- Gross alpha activity concentration on seawater

Gross alpha activity concentration for each sample and for each campaign is given in table 8. The activity concentration and the minimum detection limit is given in Bq/L.

Sample	Area	Gross- α	MDA
APLC16_1	Southern arch	0.120 ± 0.003	0.0007
APLC16_2	Peña la vieja	0.099 ± 0.004	0.0011
APLC16_3	Northern arch	0.084 ± 0.004	0.0011
APLC16_2.1	Southern arch	0.114 ± 0.005	0.0012
APLC16_2.2	Peña la vieja	0.089 ± 0.003	0.0009
APLC16_2.3	Northern arch	0.098 ± 0.003	0.0007

Table 8. Gross alpha activity and the minimum detection limit in Bq/L for each sample on each part of the beach.

As it can be observed on the southern arch gross alpha activity values are higher than on the rest of the beach with values of 0.12 ± 0.003 Bq/L for the first campaign and 0.114 ± 0.005 Bq/L on the second campaign. On the rest of the beach the values are not higher than of 0.1 Bq/L. Since the gross alpha activity presence is mainly due to uranium, specifically ^{234}U and ^{238}U , and ^{226}Ra (Degerlier, M. and Karahan, G., 2010; Otansev, P., et al., 2016) the higher value found on the southern arch could be an indicator of the presence of this element on that part of the beach and this could be due to some input of continental waters in the area of the southern arch. However, since there is not any study that gives information about this discharges water another study should be made in order to support this hypothesis. In table 9 the average value of gross alpha activity in Las Canteras beach is compared with the activities found in sea water in other parts of the world.

Location	Gross α	Reference
La Canteras beach (Spain)	0.101±0.003	This work
Adana (Turkey)	0.775±0.115	Degerliert, M. and Karahan, G., 2010
Chonburi (Thailand)	0.182±0.031	Pakkong, P., et al, 2013
Marmara sea	0.042	Otansev, P., et al, 2016
Saltpond oil field (Ghana)	20.5±7.8	Kpeglo, D.O., et al, 2016

Table 9. Average gross alpha activity values in Bq/L for sea water samples in different parts of the world.

It can be observed that the gross alpha from Chonburi in Thailand and the value of Las Canteras beach are very small. Within the rest of the values, the Marmara sea is the only place where a value smaller than the one in Las Canteras beach is found.

5.- CONCLUSIONS

1.- An assessment of the radiological environmental impacts was performed in Las Canteras beach. For this purpose the radionuclides present in samples of intertidal sand and water were evaluated. The main conclusions obtained for this analysis have been:

For sand samples:

- Mean activity concentrations of the natural radionuclides were 14.6±1.0 Bq/kg for ^{226}Ra , 17.4±1.0 Bq/kg for ^{232}Th , 528±24 Bq/kg for ^{40}K and ^{235}U was not detected.
- These obtained values in Las Canteras beach are within the normal values.
- Artificial radionuclides, specific ^{137}Cs , were not found.
- The outdoor annual effective dose in Las Canteras beach had a mean value of 0.048±0.003 mSv/y. This is below the world's average value (0.07 mSv/y).
- This study provides a useful current baseline for the detection of any future radiological alteration in Las Canteras.

For water samples:

- The mean value of gross alpha activity is 0.101±0.003 Bq/L. This value is similar to the value found in other parts of the world.
- The mean value of gross alpha activity is also similar to the mean value of uranium on seawater (0.0814 Bq/L).

2.- The activity concentration of ^{40}K on the southern arch show a significant variation between the campaign of June 2016 and the other two. This might suggest the use of ^{40}K as a tracer for the sedimentary dynamic of the beach.

3.- With respect to $^{210}\text{Pb}_{\text{ex}}$, the mean activity concentration are similar along the beach and in the different campaigns. It could indicate that the fallout is the main factor which determines the deposition of $^{210}\text{Pb}_{\text{ex}}$ along the beach.

4.- The gross alpha activities are slightly higher on the southern arch than on the other zone of the beach. This could be an indicator of the submarine ground water discharges in the southern arch.

6.- REFERENCES

- Aarkrog, A.; Dahlgard, H. and Nielsen, S.P. (1999). Marine radioactivity in the Arctic: a retrospect of environmental studies in Greeland waters with emphasis on transport of ^{90}Sr and ^{137}Cs with the East Greenland Current. *The Science of the Total Environment*, 237/238, 143-151.
- Alonso, I. and Pérez-Torrado, F.J. (1992). Estudio Sedimentológico de la playa de Las Canteras (Gran Canaria): datos preliminares. III Congreso Geológico de España y VIII Congreso Latinoamericano de Geología: Actas de las sesiones científicas. 131-135.
- Alonso, I. (1993). Procesos sedimentarios en la playa de Las Canteras (Gran Canaria). PhD. thesis. Universidad de Las Palmas de Gran Canaria.
- Alonso, I. and Vilas, F. (1996). Variabilidad sedimentaria en la playa de Las Canteras (Gran Canaria). *Geogaceta*, 20 (2), 428-430.
- Alonso, I. (2005). Costa norte: playa de Las Canteras. Tendencias actuales en geomorfología litoral: aportaciones a las III Jornadas de Geomorfología Litoral, celebradas en Las Palmas de Gran Canaria, 28-30 de abril de 2005, 219-238.
- Arnedo, M.A.; Tejera, A.; Rubiano, J.M.; Alonso, H.; Gil, J.M.; Rodríguez, R. and Martel, P. (2013). Natural radioactivity measurements of beach sands in Gran Canaria, Canary Islands (Spain). *Radiation Protection Dosiometry*. 1-12.
- Arnedo, M.A. (2014). Evaluación del fondo radiactivo natural de las Islas Canarias Orientales, implicaciones radiológicas sobre la población. PhD. thesis. Universidad de Las Palmas de Gran Canaria.
- Azouazi, M.; Ouahidi, Y.; Fakhi, S.; Andres, Y.; Abbe, J.Ch. and Benmansour, M. (2000). Natural radioactivity in phosphates, phosphogypsum and natural waters in Morocco. *Journal of Environmental Radioactivity*, 54, 231-242.
- Bonotto, D.M. (2014). ^{222}Rn , ^{220}Rn and other dissolved gases in mineral waters of southeast Brazil. *Journal of Environmental Radioactivity*, 132, 21-30.
- Casanova, M. (2015). Sedimentary budget on Las Canteras Beach, Gran Canaria (Canary Islands, Spain). Final degree work. Universidad de Las Palmas de Gran Canaria.
- Casas-Ruiz, M.; Ligeró, R.A. and Barbero, L. (2012). Estimation of annual effective dose due to natural and man-made radionuclides in the metropolitan area of the Bay of Cadiz (SW of Spain). *Radiation protection dosimetry*, 15, 60-70.
- Consejo de Seguridad Nuclear (CSN); Ministerio de Educación y Ciencia. (2004). El CSN y las radiaciones: guía del profesor. CSN, 26.
- Degerlier, M. and Karahan, G. (2010). Natural radioactivity in various surface waters in Adana, Turkey. *Desalination*, 261, 126-130.

- Déniz-González, I. y Mangas, J. (2012). Lugares de Interés Geológico en la costa de Las Palmas de Gran Canaria (Islas Canarias): inventario y valoración. *Geotemas*, 13. Sociedad Geológica de España.
- Elisha, J.J; Yisa, J. and Adeyemo, D.J. (2013). Radiological Analysis of Selected Organic Fertilizers in Zaria Local Government Area Council, Kaduna State, Nigeria: Possible Health Implications. *Journal of Applied Physics*, 5, 44-48.
- Fernández Timón, A.; Jurado Vargas, M.; Ruano Sánchez, A.B.; de la Torre Pérez, J. and Martín Sánchez, A. (2013). Influence of source composition and particle energy on the determination of gross alpha activity. *Applied Radiation and Isotopes*, 82, 376-381.
- Garzón Ruipérez, L. (1979). *Radiactividad y medioambiente*. Servicio de publicaciones Universidad de Oviedo.
- Hülse, P. and Bentley Sr, S.J. (2012). A ^{210}Pb sediment budget and granulometric record of sediment fluxes in a subarctic deltaic system: The Great Whale River, Canada. *Estuarine, Coastal and Shelf Science*, 109, 41-42.
- Karam, P.A. and Stein, B.P. (2009). *Science Foundations: Radioactivity*. New York: Chelsea House, 123.
- Kpeglo, D.O.; Mantero, J.; Darko, E.O.; Emi-Reynolds, G.; Faanu, A.; Manjón, G.; Vioque, I.; Akaho, E.H.K. and García-Tenorio, R. (2016). Radiochemical characterization of produced water from two production offshore oilfields in Ghana. *Journal of Environmental Radioactivity*, 152, 35-45.
- Livingston, H.D. (2004). *Radioactivity in the environment: Marine radioactivity*. Oxford: ELSEVIER Ltd.
- Llauradó, M.; Vallés, I.; Abelairas, A.; Alonso, A.; Díaz, M.F.; Gracia, R.; de Lucas, M.J.; Suárez, J.A. (2006). Procedimiento para la determinación de índice de actividad alfa total en muestras de agua. Métodos de coprecipitación y evaporación. Colección Informes Técnicos 11.2006. Serie Vigilancia Radiológica Ambiental. Procedimiento 1.9. Consejo de Seguridad Nuclear.
- Lu, X, and Zang, X. (2008). Measurement of natural radioactivity in beach sands from Rizhao bathing beach, China. *Radiation protection dosimetry*, 130, 385-388.
- Mabit, L.; Benmansour, M. and Walling, D.E. (2008). Comparative advantages and limitations of the fallout radionuclides ^{137}Cs , ^{210}Pb and ^7Be for assessing soil erosion and sedimentation. *Journal of Environmental Radioactivity*, 99, 1799-1807.
- Martín Sánchez, A.; Sáenz García, G. and Jurado Vargas, M. (2009). Study of self-absorption for the determination of gross alpha and beta activities in water and soil samples. *Applied Radiation and Isotopes*, 67, 817-820.
- Montaña, M.; Camacho, A.; Vallés, I. and Serrano, I. (2012). Experimental analysis of the mass efficiency curve for gross alpha activity and morphological study of the

- residue obtained by the co-precipitation method. *Applied Radiation and Isotopes*, 70, 1541-1548.
- Montaña, M.; Fons, J.; Corbacho, J.A.; Camacho, A.; Zapata-Gracia, D.; Guillen, J.; Serrano, I.; Tent, J.; Baeza, A.; Llauradó, M. and Vallés, I. (2013). A comparative experimental study of gross alpha methods in natural waters. *Journal of Environmental Radioactivity*, 118, 1-8.
- Örgün, Y.; Altinsoy, N.; Sahin, S.Y.; Güngör, Y., Gültekin, A.H.; Karahan, G. and Karacik, Z. (2007). Natural and anthropogenic radionuclides in rocks and beach sands from Ezine region (Çanakkale), Western Anatolia, Turkey. *Applied Radiation and Isotopes*, 65, 739-747.
- Ortega Aramburu, X. and Jorba Bisbal, J. (1996). *Radiaciones ionizantes: Utilización y riesgos (vol. I –II)*. Barcelona: Edicions de la Universitat Politècnica de Catalunya, SL.
- Otansev, P.; Taskin, H.; Bassari, A. and Varinlioglu, A. (2016). Distribution and environmental impacts of heavy metals and radioactivity in sediments and seawater samples of the Marmara Sea. *Chemosphere*, 154, 266-275.
- Pakkong, P.; Wongsanit, S.; Tumnoi, Y. and Udomsomporn, S. (2013). Determination of gross alpha and beta activities in seawater and plankton from the Upper Gulf of Thailand. *Journal of Radioanalytical and Nuclear Chemistry*, 297, 297-302.
- Pérez-Torrado, F.J. (1992). *Volcanoestratigrafía del Grupo Roque Nublo (Gran Canaria)*. PhD. thesis. Universidad de Las Palmas de Gran Canaria.
- Pérez-Torrado, F.J.; Calvet, F.; Cabrera, M.C. and Mangas, J. (2000). *Estudio de los depósitos litorales de la Playa de Las Canteras, Las Palmas de Gran Canaria*. Taller y Tertulias de Oceanografía, Una visión interdisciplinar de la Oceanografía. Facultad de Ciencias del Mar, Universidad de Las Palmas de Gran Canaria.
- Pope, J.A. (1989). *Options in Physics: Medical physics*. Oxford: Heinemann Educational books Ltd.
- Sanchez-Cabeza, J.A.; Díaz-Asencio, M. and Ruiz-Fernández, A.C. (2012). *Radiocronología de Sedimentos Costeros Utilizando ^{210}Pb : Modelos, Validación y Aplicaciones*. Viena: Organismo Internacional de Energía Atómica, 117.
- Suárez-Navarro, J.A.; Pujol, L.I.; and de Pablo, M.A. (2002). Rapid determination of gross alpha-activity in sea water by coprecipitation. *Journal of Radioanalytical and Nuclear Chemistry*, 253 (1), 47-52.
- Suárez-Navarro, J.A. (2009). *Investigación de procedimientos radioquímicos para la determinación de los principales emisores alfa en agua para su implementación en una red de vigilancia radiológica ambiental*. PhD. thesis. Universidad Autónoma de Madrid.

- Szmytkiewicz, A. and Zalewska, T. (2014). Sediment deposition and accumulation rates determined by sediment trap and ^{210}Pb isotope methods in the Outer Puck Bay (Baltic Sea). *OCEANOLOGIA*, 56, 85-106.
- United Nations Scientific Committee on the Effects of Atomic Radiation (UNSCEAR). (2000). Sources and effects of ionizing radiation. Report to the General Assembly with Annexes. UNSCEAR.
- Veiga, R.; Sanches, N.; Anjos, R.M.; Macario, K.; Bastos, J.; Iguatemy, M.; Aguilar, J.G.; Santos, A.M.A.; Mosquera, B.; Carvalho, C.; Baptista Filho, M. and Umisedo, N.K. (2006). Measurement of natural radioactivity in Brazilian beach sands. *Radiation Measurements*, 41, 189-196.
- Vukotic', P., Borisov, G. I., Kuzmic', V., Antovic', N., Dapc'evic', S., Uvarov, V. and Kulakov, V. M. (1998) Radioactivity on the Montenegrin Coast, Yugoslavia. *Journal of Radioanalytical and Nuclear Chemistry*, 235, 151-157.

ANNEX

Absorption curve to determine self-absorption factor.

Alpha particles, as they pass through a material medium, experiment a series of interactions with the constituent atoms of the material. In the course of these interactions the particles lose their energy until, if the material has a sufficient thickness, come to stop and electrically neutralized by capturing two electrons and they become a helium atom. The most responsible for this energy loss process is the electromagnetic interaction between the alpha particle and the atomic electrons of the medium. These interactions can be interpreted as the incident particle collisions with atomic electrons; collisions can be elastic or inelastic type. In the first case the kinetic and total energy is conserved part of the kinetic energy of the incident particle is transferred as kinetic energy of the atom. In the second case, part of the transferred energy is absorbed by the atom, which passes to an excited state or ionizes (Ortega Aramburu, X. and Jorba Bisbal, J., 1996). Self-absorption factor quantifies the efficiency loss due to the interaction of alpha particles with the final precipitate the coprecipitation method (Suárez-Navarro, J.A., 2009). For this method, ^{241}Am efficiency curves for ZnS(Ag) detector have been constructed in the course of this work with the purpose of determine how is carried out when measuring gross alpha activity by using this method. For both soils and water samples self-absorption corrections are very significant and must be introduced when the residue is important (Martin Sánchez, A., et al., 2009; Montaña M., et al., 2012; Fernández Timón, A., et al., 2013).

To create the alpha absorption curves different patterns have been prepared with different mass thickness according to Llauradó, M., et al., (2006). The process for preparing patterns absorption has been to perform the coprecipitation method with a constant and known quantity of ^{241}Am and a variation in the amounts of carrier used, with a constant increase in the volume of both carriers in a range of 1 to 2 mL. So the starting point was the one made with 1 mL of carrier barium and 1 mL of carrier iron as these will be the amounts used in the coprecipitation method and will serve for the detection efficiency for this method.

Absorption curve was realized with six points which were prepared in triplicate in order to have adequate statistics. Each point added 0.2 ml more of carriers than the one before. The range of the weights obtained is between 17 and 35 mg.

To calculate the efficiency of the counting on each point created (E) the following equation was used:

$$E = \frac{cpm_{alpha} - cpmb_{alpha}}{dpm_{pattern}} \quad (16)$$

where cpm_{alpha} is the alpha counting rate of the ^{241}Am pattern sample prepared in counts per minute, $cpmb_{alpha}$ is the alpha counting rate of the reference sample also in counts per minute and $dpm_{pattern}$ correspond to the decays per minute of the ^{241}Am pattern sample prepared. Self-absorption factor (F_i) for each point of the curve was calculated with the next equation:

$$F_i = \frac{E_i}{E} \quad (17)$$

where E_i is the efficiency of the counting for each point of the curve and E is the efficiency of the counting for the first sample of ^{241}Am pattern prepared with 1 ml of barium and iron carrier.

The mean values calculated for precipitate mass thickness, average mas of tracer, efficiency of counting and auto absorption factor are shown on table 10.

Point	Δp (mg)	Tracer mass (mg)	Fa	E (%)
Am10_16	18.40	0.86	1.00	31.64
Am12_16	20.97	0.87	0.88	27.96
Am14_16	25.27	0.86	0.77	24.19
Am16_16	26.93	0.86	0.77	24.35
Am18_16	30.23	0.86	0.68	21.60
Am20_16	34.33	0.87	0.64	20.06

Table 10. Mean values of precipitate mass thickness (Δp), average tracer mass, auto absorption factor (Fa) and efficiency of counting (E).

Absorption curve was made for the ZnS(Ag) detector with the self-absorption factors obtained for each point and the mass thickness values (Figure 10). Due to the variety of settings used the quadratic fit was selected as the trend of the curve is not linear. Thus the quadratic polynomial for determining self-absorption factor is:

$$fa = 0.0009x^2 - 0.0696x + 1.9632 \quad (18)$$

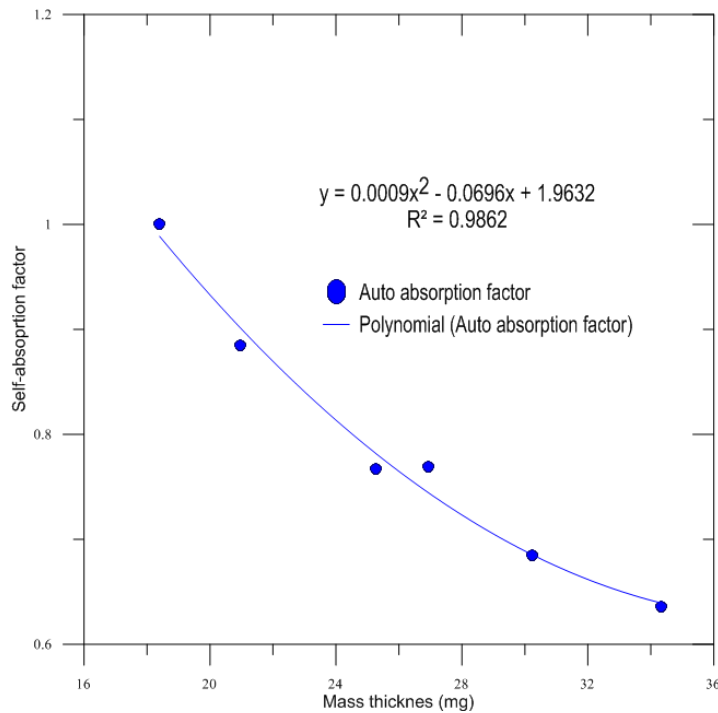


Figure 10. Absorption curve.

VALORACIÓN PERSONAL (PERSONAL ASSESSMENT)

1. *Actividades desarrolladas durante la realización del TFT*

Durante la realización del Trabajo de Fin de Título se desarrollaron distintos tipos de trabajos, algunos de los cuales estaban incluidos en las prácticas externas. Por un lado se planificaron y realizaron tres recogidas de muestras de arena (en octubre de 2015, enero de 2016 y en mayo de 2016) y dos recogidas de muestras de agua (en enero de 2016 y en abril de 2016), todas ellas de la Playa de Las Canteras. También se realizó el tratamiento de cada una de las muestras para la posterior medida de las emisiones gamma en las muestras de arena y alfa total en las muestras de agua. Después se realizó el tratamiento y análisis adecuados de los datos obtenidos a partir de las muestras recogidas y analizadas.

Por otro lado durante las prácticas también se desarrolló una curva de auto absorción que posteriormente se utilizaría para determinar la eficiencia del aparato, así como el factor de auto-absorción de las muestras que se medirían en dicho aparato (como se encuentra indicado en el apartado “Annex”). Para desarrollar la curva de auto-absorción se realizó el mismo proceso químico que se llevó a cabo en las muestras de agua recogidas (tal y como se describe en el apartado “Material and methods” de este documento). Finalmente también se realizó una búsqueda bibliográfica sobre el tema a tratar en el TFT y paralelamente a la realización de los experimentos se realizó la redacción del mismo.

2. *Formación recibida*

Durante el segundo semestre del curso 2015-16, dentro del Máster Interuniversitario en Oceanografía se impartió la asignatura Oceanografía a Gran Escala y Mesoscala, donde se incluyó el tema **Radioactividad Marina**, siendo éste el IV tema de la asignatura. Esta lección constó de cuatro sesiones teóricas: la primera, *Radioactividad. Radiaciones ionizantes*; la segunda, *Interacción de las radiaciones ionizantes con la materia. Detección, medida y unidades de las radiaciones*; la tercera, *Radiaciones ionizantes en el medio ambiente. Radionúclidos en el medio marino* y la cuarta *Aplicaciones y casos de estudio aplicados al medio marino*. Al ser sesiones relacionadas con mis prácticas externas y mi TFT se me brindó la oportunidad de asistir a modo de libre oyente. Además puede asistir, también en calidad de libre oyente, a las tres sesiones de prácticas planificadas, *Cartas de Nucleídos. Desintegración radiactiva: Equilibrios; Determinación de alfa total en agua de mar y Espectroscopía alfa (Po-210 en muestras marinas)*. Todo ello me ha servido para profundizar en los aspectos teóricos y prácticos que he desarrollado para la realización de las prácticas externas y el TFT en el ámbito de la Radiactividad Ambiental aplicada al entorno marino.

3. *Nivel de integración e implicación dentro del departamento y relación con el personal.*

El nivel de integración dentro del departamento se puede considerar como bastante bueno. Desde el primer día se me ha facilitado todo tipo de ayuda tanto en forma de contenido bibliográfico, así como recomendaciones personales para el buen

desarrollo del TFT. Mi incorporación fue inmediata, realizando sin problema las tareas que se me encomendaron y colaborando en cualquier oportunidad que se me presentase. Aunque no he tenido la ocasión de conocer en persona a todos los miembros del grupo de investigación cabe destacar que, siguiendo un sistema de cordialidad y mutuo respeto, la relación con el resto de integrantes del grupo ha sido buena, sin tener ningún incidente con ninguno de los miembros que he llegado a conocer.

4. Aspectos positivos y negativos más significativos relacionados con el desarrollo del TFT

Entre los aspectos positivos de la realización del TFT cabría destacar que la realización del mismo brinda la oportunidad para el alumno de conocer cómo se desarrollaría la elaboración de un trabajo de investigación. De esta manera se plantea una posibilidad de conocer mejor lo que nos espera en el mundo laboral, así como un entrenamiento para trabajar la autonomía de cada uno a la hora de desarrollar un trabajo de forma relativamente independiente. Además presenta la oportunidad de ampliar los conocimientos de los alumnos en las áreas determinadas de interés de cada uno, así como la posibilidad de entrenar y mejorar la forma de desenvolverse en un idioma distinto al materno.

Entre los aspectos negativos destacaría la dificultad que supone el tener que desarrollar el proyecto en inglés, sobre todo para aquellos alumnos que tengan problemas para desenvolverse en dicho idioma. Además, también sería interesante comentar que en comparación con las prácticas externas, la información que se facilita sobre los documentos que deben ser rellenados tanto por tutores como alumnos es bastante más reducida. Por último destacaría los plazos de entrega de los TFT ya que, aunque durante el cuatrimestre hay bastante tiempo, si el alumno tiene alguna asignatura pendiente a cursar durante el segundo cuatrimestre o para examinarse en la convocatoria extraordinaria de Julio, el margen de tiempo que queda para la realización del proyecto se ve bastante reducido, teniendo en cuenta que no estamos acostumbrados a la realización de proyectos de esta magnitud.

5. Valoración personal del aprendizaje conseguido a lo largo del TFT

La posibilidad que se presenta con el TFT de trabajar en áreas más especializadas facilita el aprender y afianzar más y mejor los conocimientos de la misma. Esto quiere decir que al realizar el TFT junto a las prácticas externas he podido aprender más en profundidad las bases teóricas prácticas del tema a tratar, en mi caso la radiactividad ambiental. También destacaría la posibilidad de trabajar de forma independiente tanto en un muestreo como en un laboratorio, aprendiendo distintas técnicas, así como distintas respuestas ante dificultades y problemas que se presentan a la hora de realizar los mismos. Así mismo destacaría el aprendizaje a la hora de tratar y analizar los datos obtenidos tras un trabajo experimental. Además valoraría positivamente la mejora a la hora de realizar búsqueda de fuentes bibliográficas, así como el análisis y síntesis del contenido de las mismas. Por último destacar el aprendizaje obtenido a la hora de estructurar y redactar un proyecto de investigación científica. De esta manera se ha fomentado y mejorando mi autonomía y responsabilidad de cara al mundo laboral.